Electron Dynamics in Magnetosheath Mirror-Mode Structures

S. T. Yao[1,2] , Q. Q. Shi[1] , J. Liu[2], Z. H. Yao[3,4] , R. L. Guo[5] , N. Ahmadi[6] , A. W. Degeling[1] , Q. G. Zong[7] , X. G. Wang[8] , A. M. Tian[1] , C. T. Russell[9] , H. S. Fu[10] , Z. Y. Pu[7] , S. Y. Fu[7] , H. Zhang[11] , W. J. Sun[5] , L. Li[7] , C. J. Xiao[12], Y. Y. Feng[2], and B. L. Giles[13]

[1]Shandong Provincial Key Laboratory of Optical Astronomy and Solar-Terrestrial Environment, Institute of Space Sciences, Shandong University, Weihai, China, [2]State Key Laboratory of Space Weather, National Space Science Center, Chinese Academy of Sciences, Beijing, China, [3]Mullard Space Science Laboratory, University College London, Dorking, UK, [4]Laboratoire de Physique Atmosphérique et Planétaire, STAR Institute, Université de Liège, Liège, Belgium, [5]Key Laboratory of Earth and Planetary Physics, Institute of Geology and Geophysics, Chinese Academy of Sciences, Beijing, China, [6]Laboratory for Atmospheric and Space Physics, University of Colorado Boulder, Boulder, CO, USA, [7]School of Earth and Space Sciences, Peking University, Beijing, China, [8]Department of Physics, Harbin Institute of Technology, Harbin, China, [9]Department of Earth, Planetary and Space Sciences, University of California, Los Angeles, CA, USA, [10]School of Space and Environment, Beihang University, Beijing, China, [11]Physics Department and Geophysical Institute, University of Alaska Fairbanks, Fairbanks, AK, USA, [12]State Key Laboratory of Nuclear Physics and Technology, School of Physics, Peking University, Beijing, China, [13]NASA Goddard Space Flight Center, Greenbelt, MD, USA

Abstract Mirror-mode structures are widely observed in space plasma environments. Although plasma features within the structures have been extensively investigated in theoretical models and numerical simulations, relatively few observational studies have been made, due to a lack of high-cadence measurements of particle distributions in previous space missions. In this work, electron dynamics associated with mirror-mode structures are studied based on Magnetospheric Multiscale observations of electron pitch angle distributions. We define mirror-mode peaks/troughs as the region where the magnetic field strength is greater/smaller than the mean field. The observations show that most electrons are trapped inside the mirror-mode troughs and display a donut-like pitch angle distribution configuration. Besides the trapped electrons in mirror-mode troughs, we find that electrons are also trapped between ambient mirror-mode peaks and coexisting untrapped electrons within the mirror-mode structure. Analysis shows that the observed donut-like electron distributions are the result of betatron cooling and the spatial dependence of electron pitch angles within the structure.

1. Introduction

The mirror-mode structure is a fundamental feature in space plasmas. It has been observed in solar wind (Tsurutani et al., 1992; Yao et al., 2013), planetary magnetosheath (e.g., Balikhin et al., 2009, 2010; Joy et al., 2006; Soucek et al., 2008; Tsurutani et al., 1984), cometary comas (Russell et al., 1987), and heliosheath (Burlaga et al., 2006) plasmas. This structure, which is stationary in the plasma rest frame, displays anticorrelation between magnetic field strength and plasma pressure. Previous studies have revealed that the mirror-mode structures are generated in high plasma beta (the ratio of the plasma pressure to the magnetic pressure) regions, with the perpendicular plasma pressure being greater than parallel plasma pressure. They were also often considered a possible source of magnetic dips in many studies (e.g., Ahmadi et al., 2017; Horbury et al., 2004; Joy et al., 2006; Shi et al., 2009; Xiao et al., 2014; Zhang et al., 2008), though different mechanisms were proposed by others (e.g., Balikhin et al., 2012; Ji et al., 2014; Li et al., 2016; Yao et al., 2016, 2017, 2018). Furthermore, their spatiotemporal scales and evolution processes, three-dimensional (3-D) structures, and other important kinetic effects (e.g., drift, finite Larmor radius effect, non-Maxwellian ion distribution, and electron temperature influence) were also extensively investigated (e.g., Ahmadi et al., 2016; Chisham et al., 1998; Feygin et al., 2009; Gary & Karimabadi, 2006; Gedalin et al., 2001; Genot et al., 2009; Hasegawa, 1969; Hellinger et al., 2009; Klimushkin & Chen, 2006; Pokhotelov et al., 2013; Pokhotelov & Pilipenko, 1976; Treumann et al., 2004). Nevertheless, previous studies were mostly limited by the measurement resolution of on board instruments that is particularly important to understanding of microphysics at the ion gyroscale or even the electron dynamics scale.

In a theoretical treatment of dynamics, Southwood and Kivelson (1993) investigated the linear stage of the mirror mode and suggested that the mirror-mode instability was controlled by particles with a slow

parallel velocity, named *resonant* particles. Subsequently, the nonlinear stage of the mirror mode was then studied by Kivelson and Southwood (1996). In their study, particle distributions were divided into trapped and untrapped populations, corresponding to the magnetic field variations. The trapped particles were further divided into shallowly trapped (with their pitch angle close to the loss cone edge) and deeply trapped (with the pitch angle nearly 90°). During the development of magnetic troughs and peaks, the deeply or shallowly trapped particles would encounter their mirror points diverging and converging, respectively. They hence lost or gained energy by Fermi deceleration or acceleration, respectively. As the magnetic trough became deeper, the deeply trapped particles were further cooled via betatron mechanisms (e.g., Fu et al., 2011, 2012, 2013; Konjukov & Terietskij, 1958; Liu et al., 2017; Northrop, 1963). These processes then resulted in a distribution function with particles to be cooled at nearly perpendicular pitch angles and heated at intermediate pitch angles. Chisham et al. (1998) studied behaviors of the mirror-mode electron distribution in the terrestrial magnetosheath. Within the mirror-mode troughs, observations have shown that the deeply trapped electrons are cooled and the shallowly trapped electrons are heated with respect to the rest of the electron velocity distributions. This was explained by Fermi acceleration/deceleration and betatron deceleration mechanisms. Recently, Soucek and Escoubet (2011) performed detailed analysis on measurements of trapped ions associated with mirror-mode structures in the magnetosheath. In this study, Cluster data were used to confirm the relation between the ion pitch angle and the magnetic field variation, predicted earlier by Southwood and Kivelson (1993).

Historically, electron distributions have not been well analyzed in observational studies, due to the insufficient resolution of spacecraft instrumentation. The high-resolution data currently available from the Magnetospheric Multiscale (MMS) mission provide an excellent opportunity to study the electron distribution within mirror-mode structures. In this study, we show the details of electron pitch angle distributions (PADs) using MMS data, which resemble a donut-like configuration. Further analysis indicates that this feature is closely linked to several important physical processes. This paper is organized as follows. Details of observations are shown in section 2. Then in section 3, we discuss the potential generation mechanisms of the electron donut-like distributions. In subsection 3.1, the betatron cooling effect on electrons is studied; and in sub section 3.2, we show that the spatial variation of electron pitch angles along their trajectories also plays an important role in formation of a donut-like distribution. The paper is then concluded by a summary and discussion section.

2. Observations

Recent MMS mission (Burch et al., 2015) provides an ideal opportunity to investigate details of electron distributions in the mirror-mode structures. In this study we use magnetic field data from Fluxgate Magnetometer instrument (Russell et al., 2016) that has a sampling rate of 128 Hz in burst mode and 16 Hz in survey mode, and ion/electron data from Fast Plasma Investigation instrument (Pollock et al., 2016) that has a resolution of 4.5 s in fast mode and 150 ms (30 ms) for ions (electrons) in burst mode.

Figure 1 is an overview plot of observed mirror-mode structures in the magnetosheath observed on 10 September 2015. The first two panels show the ion and electron energy spectra. The remaining panels show the magnitude and three vector components of the magnetic field in Geocentric Solar Ecliptic coordinates (c), and the ion number density (d), bulk velocity (e), and parallel and perpendicular temperatures (f) of ions, as well as the electron parallel and perpendicular temperatures (g), observed by MMS1. The MMS spacecraft were located at about [1.7, 11.5, −0.5] R_E (Earth radii) in the magnetosheath and crossed the magnetopause at ~19:16:00 UT. From Figure 1c we can find a sequence of mirror-mode structures during an interval of ~25 min (between the two dashed gray lines). The plasma properties also change in concert with the magnetic field during this interval. Figures 2a–2e present the details of the mirror-mode structures. The *z* component of magnetic field shows the most significant variations, with both ion and electron number densities varying in antiphase to the total magnetic field strength. The ion temperature is anisotropic (with the ratio of the perpendicular to the parallel components ~1.25). The electron temperature is also anisotropic but weaker than that of the ions. The magnetic pressure (P_b) and thermal pressure (P_t, including both ion and electron contributions) are plotted in Figure 2e. The total pressure ($P = P_t + P_b$) also shown in Figure 2e exhibits much smaller-scale variations than either P_t or P_b (which are strongly anticorrelated), indicating that these mirror-mode structures are approximately pressure balanced.
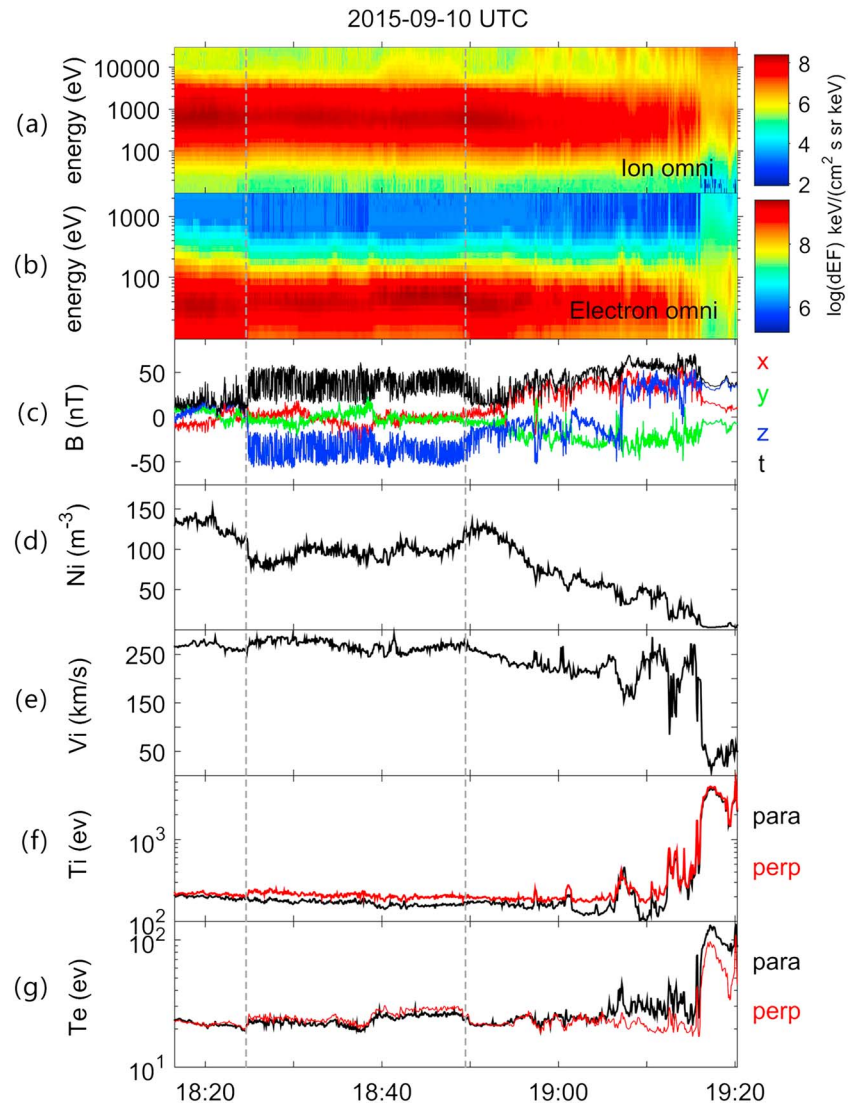
Figure 1. Overview plot from MMS1 observations. (a and b) Ion and electron differential energy fluxes. (c) Magnetic field components in the GSE coordinates and total field strength. (d) Ion number density. (e) Ion bulk velocity. (f) Ion parallel and perpendicular temperature. (g) Electron parallel and perpendicular temperature. MMS = Magnetospheric Multiscale; GSE = Geocentric Solar Ecliptic.

Figure 3 presents electron PADs of the mirror-mode structures shown in Figure 2. The maximum, average, and minimum magnetic field strengths (B_{max}, B_{ave}, B_{min}) over the interval are 56.3, 36.8, and 17.2 nT, respectively, shown by the dotted line in Figure 3a. We assume B_{ave} approximates the background magnetic field strength B_{bg}. To distinguish peaks from troughs for the mirror-mode structures, we define the peaks as the region where the magnetic field strength is greater than B_{bg}, and the troughs as the region where the magnetic field strength is less than B_{bg}. Under this definition, similar to that in Kivelson and Southwood (1996), Chisham et al. (1998), and Soucek and Escoubet (2011), it is reasonable to assume that the peaks and troughs are developed on the basis of B_{bg} (see, e.g., Balikhin et al., 2009; Kivelson & Southwood, 1996). As these peaks and troughs increase in amplitude, particles are increasingly excluded from the strong field regions (peaks) and trapped within weak field regions (troughs).

Figures 3b–3g display the electron PADs from 41 eV to 3,779 eV. Several instances of donut-like distributions, coinciding with the magnetic trough locations, are clearly visible in the plots. A function of $\sin \theta = \sqrt{B/B_{bg}}$, where B is the local magnetic field strength, is applied to obtain the loss cone angle θ for the mirror-mode troughs, and is also considered to be the critical trapped angle (CTA) of the particles. It can be found that
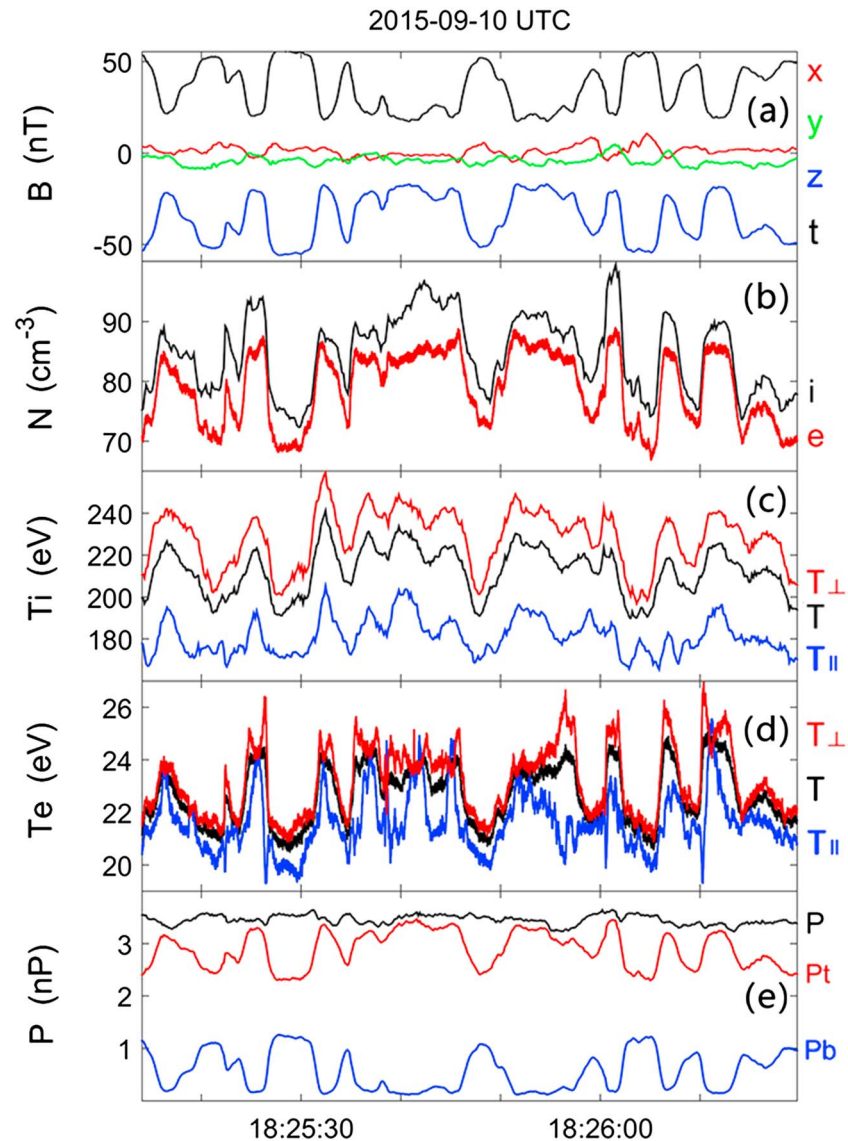
Figure 2. MMS1 detailed observations of mirror-mode structures. (a) Magnetic field components in GSE coordinates and total field strength. (b) Ion and electron number density. (c and d) Ion and electron temperature. (e) Magnetic pressure (blue), thermal pressure (red), and their sum (black). MMS = Magnetospheric Multiscale; GSE = Geocentric Solar Ecliptic.

the CTA, shown as the solid black line, matches well with the donut distributions. Figures 3i and 3k show details of the donut distributions for 52 eV electrons, from 18:25:23 UT to 18:25:28 UT and from 18:25:59.2 UT to 18:26:03.5 UT, respectively. The pitch angle resolution is 15° (i.e., 12 bins from 0° to 180°). With such a resolution, the donut-like distribution fits well within the CTA. Also we plot the CTA with $\sin\theta = \sqrt{B/B_{max}}$. The results are shown by the dashed black line. One can find that a few electrons are trapped between the dashed and solid lines. This may imply that (1) most of electrons are trapped in the mirror-mode troughs; (2) for the remaining electrons, some of them are still trapped among the ambient mirror-mode peaks; (3) while the others, that is, the electrons with a large parallel velocity at B_{min}, are untrapped in the mirror-mode troughs or peaks.

3. Possible Formation Mechanisms

3.1. Betatron Cooling

Previous studies have predicted that particles at intermediate pitch angles are heated by Fermi acceleration, while the deeply trapped particles are cooled by Fermi and betatron deceleration (e.g., Chisham et al., 1998;

Figure 3. Electron pitch angle distributions from MMS1. (a) Magnetic field strength. Three gray horizontal lines indicate the maximum, mean, and minimum magnetic field strength during this time interval. (b–g) Electron pitch angle distributions. The black lines are the trapped critical angle. (h–k) Details of the pitch angle distributions of 52 eV electrons and their corresponding magnetic field strength. The black solid a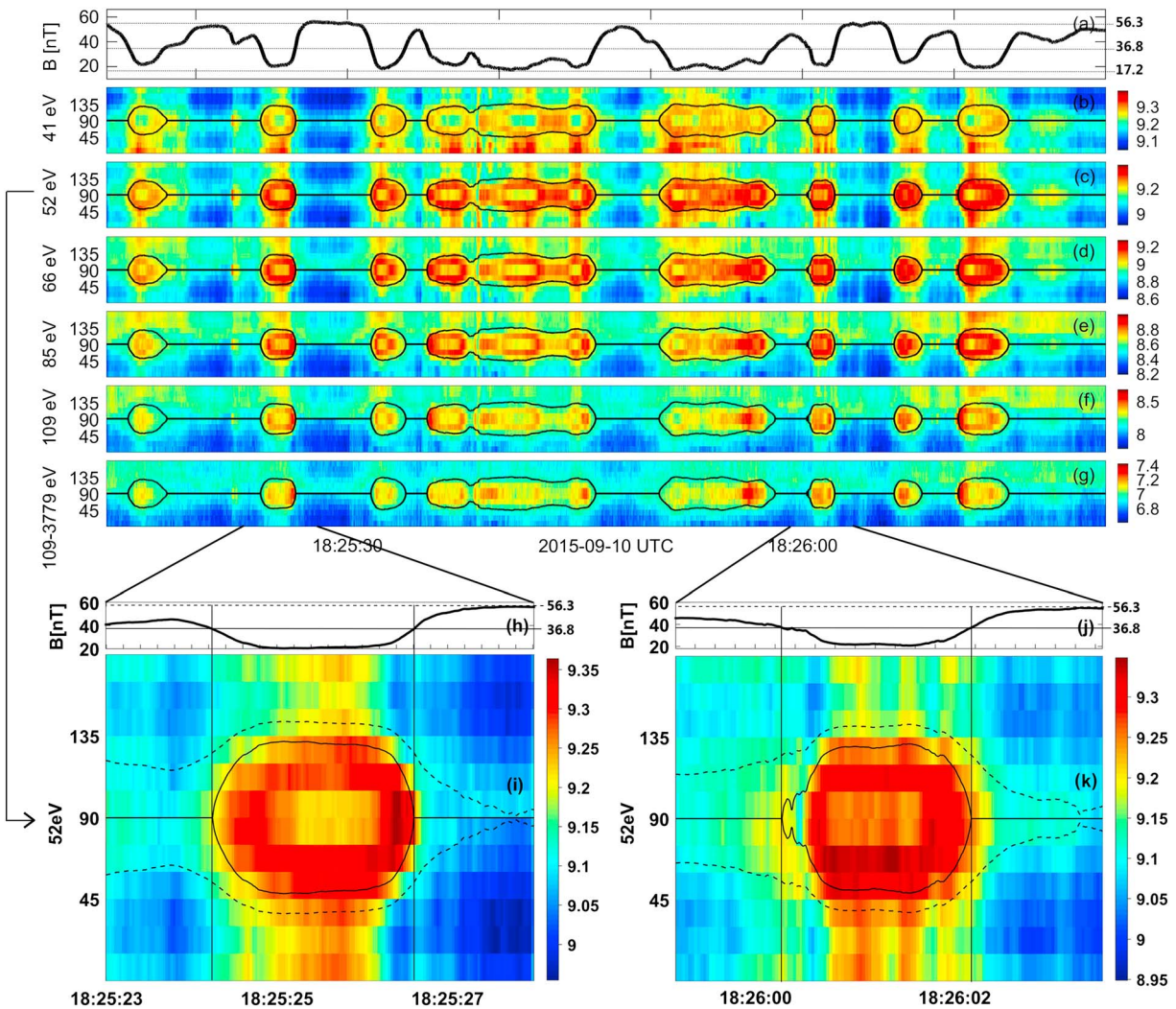nd dashed lines are the critical trapped angles calculated from the mean and maximum magnetic field strength, respectively.

Kivelson & Southwood, 1996). However, in the analysis of in situ measurements, it is not straightforward to evaluate the evolution of the mirror-mode structure. For example, it is unclear whether they evolve from a small size and a low amplitude to a larger size and a higher amplitude, or to a smaller size but a larger amplitude. Furthermore, they may also evolve from a large size but a low-amplitude structure. More observational evidence is required to verify which of these conjectures are correct. It is therefore difficult to conclude whether or not an in situ measured signature is caused by the contraction or expansion of a structure, namely by Fermi acceleration or deceleration.

Nonetheless, since the magnetic trough becomes deeper (B_{min} becomes smaller), it would be reasonable to assume that the particles experience a cooling process via betatron deceleration. The process is quantified using $\Delta W_\perp = W_\perp \frac{\Delta B}{B}$ under the condition of magnetic moment conservation, where $W_\perp$ is the perpendicular particle energy, and B is the magnetic field strength. In Figure 4a, we depict the mirror-mode trapped particle distributions (the black line) using a cartoon in order to demonstrate the following points. For particles with a given energy, betatron cooling is more effective on particles with a pitch angle close to 90°. Thus, as illustrated in Figure 4a, the particles with a pitch angle from 90° to 75° will lose more energy than that from 75° to 60°. If we plot the PAD for a given energy, for example, the red line in Figure 4a, the particle energy
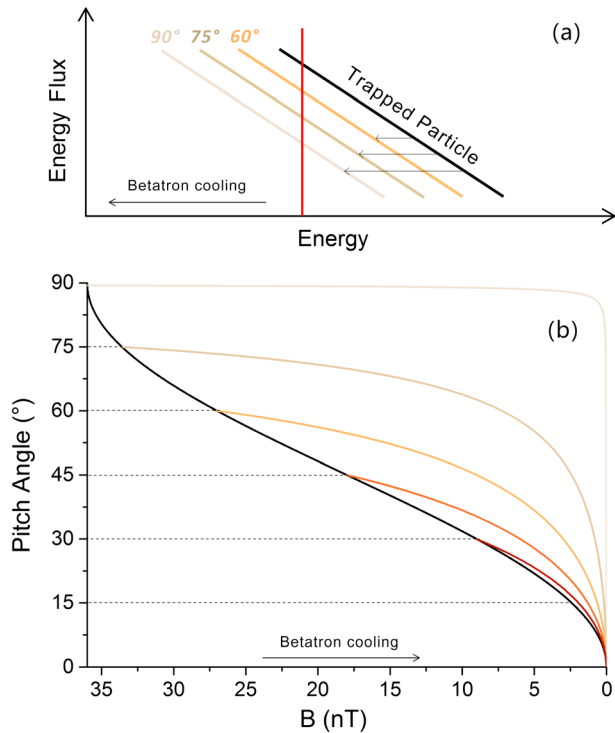
flux with the pitch angle from 90° to 75° will less than that from 75° to 60°. This inference fits well with the observations shown in Figure 3.

It is also worth noting that the particle pitch angle changes during the cooling process since their perpendicular energy is decreasing. To illustrate this, we plot the relation between the loss cone angle and the minimum magnetic field, given by $\sin\theta = \sqrt{B/B_{bg}}$ in the magnetic trough during the cooling process. Therefore, in Figure 4b, the region below the black curve can be considered as the loss cone. When the magnetic trough becomes deeper, the loss cone shrinks, with a wider range of particles becoming trapped. We calculate the pitch angle of these particles under the influence of betatron cooling, and the results are shown by shaded orange lines. It is then found that the change in loss cone is always faster than the change in the particle pitch angle. Thus, although their pitch angles are reduced by the cooling process, the particles remain trapped in the deeper mirror structure with a smaller loss cone.

3.2. Electron Dynamic in the Mirror Structure

By considering the first adiabatic invariant and kinetic energy, electrons trapped in a magnetic mirror will have larger pitch angles when moving into stronger field regions and then increase their perpendicular energy $W_\perp$. Thus, $W_\perp$ is maximal at the mirror point and $W_\parallel$ is maximal at the magnetic field minimum. When all the electrons are taken into account, we find that the perpendicular electron flux is intensified near the mirror point and decreased away from it. If the MMS spacecraft move across the mirror structure along a field line, the donut-like distribution then will be observed. However, along various field lines, the loss cones are different. For example, in the cartoon plot (Figure 5), the loss cones are ~45°, ~60°, and ~75° for Lines 1, 2, and 3, respectively.

Figure 4. (a) Schematic of the betatron cooling effect. The effects of betatron cooling are different for different pitch angle electrons. Thus, they have different motions in the horizontal axis. The red vertical line is for reference. (b) Relation between B and θ obtained from $\sin\theta = \sqrt{B/B_{bg}}$ (black curve line), where B_{bg} is 36.8 nT. The colored curves are the change in pitch angle for trapped electrons caused by betatron cooling versus B.

For Line 4, only are the particles with their pitch angle near 90° are trapped. Therefore, if the spacecraft perpendicularly crosses the field lines from B_{bg} (B_{max}) to B_{min}, then back to B_{bg} (B_{max}), a donut-like distribution will be observed, but it is set up by many different *donut* distributions in different field lines. In this study, the angle between the spacecraft trajectory and magnetic field line is ~90°. This is nearly a perpendicular
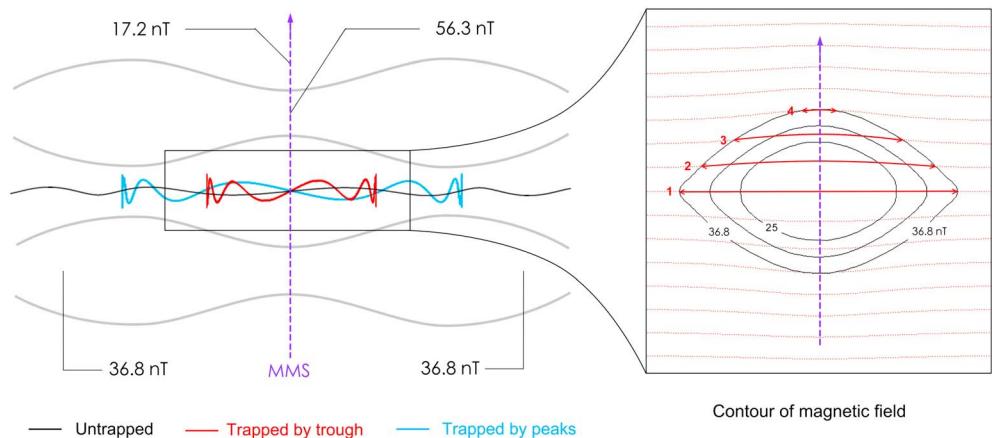
Figure 5. Schematic for the mirror-mode structures. (left) Particles trapped by the trough are denoted by the red curve, particles trapped by peaks are represented by the blue curve, and untrapped particles are represented by the black curve. (right) The red dotted lines are magnetic field lines. Numbers *1* to *4* are field line labels, and the black circles are the contours of magnetic field strength. Red arrows indicate that particles reflect from their mirror points. MMS = Magnetospheric Multiscale.

crossing, as drawn in Figure 5. Thus, the above prediction fits well with our observation and therefore is a possible formation mechanism of the donut-like distribution.

4. Summary and Discussion

In this study, we analyze the high cadence particle distribution measured by the MMS spacecraft and discuss in detail the electron PAD that shows a donut-like configuration. These observations demonstrate that most electrons are trapped within the mirror-mode troughs. Parts of the remaining electrons are trapped among the ambient mirror-mode peaks, and the rest are untrapped by mirror-mode structures. Further analysis shows that betatron cooling plays an important role in the donut-like distribution formation. Low-energy electron contribution in betatron cooling is more than higher-energy population since they have a larger population. Also the trapped electrons have their maximum perpendicular energy at mirror points and the maximum parallel energy at B_{min}. This also helps to form the electron donut-like distribution.

The possible formation mechanisms for donut-like electron PADs discussed in section 3 are also relevant to ion distributions. Soucek and Escoubet (2011) studied ion PADs in magnetosheath mirror-mode structures. The ion PADs in their study displayed features similar to donut-like electron PADs revealed in this work. Thus, ions and electrons should experience a similar physical process, that is, the possible formation mechanisms discussed in section 3. It is worth noting that when studying the field-particle relation, we usually require the distribution function (e.g., velocity and pitch angle) in the plasma flow frame but not in the spacecraft frame. This is because an observed particle distribution becomes considerably distorted when the thermal velocity is close to or smaller than the plasma bulk flow velocity (with respect to the spacecraft). This presents a fundamental problem for the analysis of particle distributions. For example, in Soucek and Escoubet (2011), the ion distributions up to 1 keV are significantly affected by the bulk plasma flow. To remove this influence, they rebinned the 3-D distributions to 2-D PADs, transforming them to the plasma flow frame in the process. Finally, the ion PADs were well resolved in their study. In principle one may expect to encounter the same problem for electrons. However, in our study the thermal velocity of the electrons of interest is 10 times greater than the plasma flow velocity. Therefore, the effect of this problem is negligible in our case.

In previous theoretical studies, a linear mirror-mode model with cold electrons was presented by Southwood and Kivelson (1993) based on the conservation of magnetic moment and different behaviors of trapped and untrapped ions. The ions primarily control the mirror-mode formation process, and the electrons should react to the ion density distribution to preserve quasi-neutrality. In our study, the observed donut-like electron distributions are similar to those of ions shown in Soucek and Escoubet (2011), which implies that the ions and electrons experience a similar physical process. Since the electron temperature in our case is only ~1/10 the ion temperature, we suspect that the Southwood and Kivelson (1993) theory is applicable here, at least in the sense that the ions are responsible for the mirror formation, and the electrons respond to the mirror structure.

The Southwood and Kivelson (1993) model was extended by Pantellini and Schwartz (1995) by taking into account an isotropic distribution of electrons with a temperature of the same order as the proton temperature. It was shown that the growth rate of the mirror mode is reduced by a longitudinal electric field that is caused by nonzero temperature electrons. This effect was also studied by quasi-linear theory (Istomin et al., 2009; Pokhotelov et al., 2000). We are currently investigating how the available observations may best be used to test these theories and hope to address this in future work. A further question is whether modifications in numerical simulations and theoretical study should be made based on the new observations, and what would be the impact of these modifications. For example, the observed doughnut-like electron distributions appear to be outside the scope of the above theoretical treatments.

Furthermore, it was previously suggested by Soucek et al. (2008) that these mirror-mode structures ranged from quasi-sinusoidal oscillations to coherent structures as magnetic troughs or peaks. The magnetic troughs were observed in a mirror stable or marginally mirror stable environment, while peaks were most likely seen where the plasma was mirror unstable. An abrupt transition from peaks to troughs near the magnetopause was identified and was interpreted as a consequence of plasma expansion, which changed the local stability of the plasma to mirror stable in the vicinity of magnetopause. The early models (Kivelson & Southwood, 1996; Pantellini, 1998) were constructed to explain the existence of magnetic troughs based on the cooling of trapped particles. Based on a hybrid simulation of the Vlasov-Maxwell equations, the nonlinear evolutions of mirror-mode structures were found to lead to magnetic peaks (Califano et al., 2008). The simulation also

showed the transition from magnetic peaks into troughs when the plasma became marginally mirror stable. Later, gyrokinetic approach was used to simulate the nonlinear growth of the mirror mode by Porazik and Johnson (2013a, 2013b). Their simulations show that magnetic troughs saturate at lower amplitude and earlier than the peaks and in turn lead to the development of magnetic peaks. To summarize, the evolution of mirror-mode structures remains a topic of active investigation. Understanding the role that electrons are playing in the evolution of mirror-mode structures remains an important question. As is well known, spacecraft measurements are only able to provide a brief glimpse as they rapidly transit across these structures and are unable to monitor the evolution of a specific structure on long timescales. Hence, to investigate the structure evolution by means of observation is still difficult. Nevertheless, we provide an electron PADs observation of a magnetic trough train in the supporting information. Similar electron donut-like distributions can be observed in these magnetic troughs, which could be the later stage of mirror-mode structure. Also, some differences can be found in the parallel and antiparallel energy flux between these troughs and the observation shown in Figure 3. This could be because the location of these troughs is very close to the magnetopause, which agrees with the inference of Soucek et al. (2008). More observation studies are needed to compare with previous theoretical and numerical simulation studies.

In Kivelson and Southwood (1996), the velocity distribution was used to illustrate the betatron cooling process. Their study also theoretically investigated the divergence and convergence of mirror points during the development of magnetic troughs and peaks. For the deeply trapped particles, since the mirror points are diverging, they lose energy due to Fermi deceleration. For the shallowly trapped particles, the mirror point is converging, resulting in heating by Fermi acceleration. In our study, it is difficult to determine how the mirror-mode structures evolve. Fermi acceleration or deceleration is more effective for particles with high parallel velocities. Hence, even if Fermi deceleration for the deeply trapped particles exists, it is not efficient and is not obvious in the observations. If the shallowly trapped particles are heated by Fermi acceleration, their energy flux will increase in the PAD. This is because the populations of low-energy particles are higher than high-energy particles. Shallowly trapped particles at a given energy are heated to a higher energy, and more shallowly trapped particles are heated from lower energy to this energy. We can confirm the energy flux increase in the PAD plots in Figure 3. However, from the theoretical viewpoint, cooling, heating, and other electron dynamic behaviors may all possibly produce a donut-like distribution. These effects may thus overlap one another. Therefore, further work should be done on evolutions of the mirror-mode structure in observations. For instance, we use multipoint spacecraft techniques (e.g., Russell et al., 1983; Shi et al., 2005, 2006) to determine expanding or contracting features of the mirror-mode structure, find the evidence of electric field variations when the magnetic structures change, and discover the relation among magnetic, thermal, and dynamic pressures, in order to examine pressure balance.

References

Ahmadi, N., Germaschewski, K., & Raeder, J. (2016). Effects of electron temperature anisotropy on proton mirror instability evolution. *Journal of Geophysical Research: Space Physics*, *121*, 5350–5365. https://doi.org/10.1002/2016JA022429

Ahmadi, N., Germaschewski, K., & Raeder, J. (2017). Simulation of observed magnetic holes in the magnetosheath. *Physics of Plasmas*, *24*, 122,121. https://doi.org/10.1063/1.5003017

Balikhin, M. A., Pokhotelov, O. A., Walker, S. N., Boynton, R. J., & Beloff, N. (2010). Mirror mode peaks: THEMIS observations versus theories. *Geophysical Research Letters*, *37*, L05104. https://doi.org/10.1029/2009GL042090

Balikhin, M. A., Sagdeev, R. Z., Walker, S. N., Pokhotelov, O. A., Sibeck, D. G., Beloff, N., & Dudnikova, G. (2009). THEMIS observations of mirror structures: Magnetic holes and instability threshold. *Geophysical Research Letters*, *36*, L03105. https://doi.org/10.1029/2008GL036923

Balikhin, M. A., Sibeck, D. G., Runov, A., & Walker, S. N. (2012). Magnetic holes in the vicinity of dipolarization fronts: Mirror or tearing structures. *Journal of Geophysical Research*, *117*, A08229. https://doi.org/10.1029/2012JA017552

Burch, J. L., Moore, T. E., Torbert, R. B., & Giles, B. L. (2015). Magnetospheric multiscale overview and science objectives. *Space Science Reviews*, *1–17*. https://doi.org/10.1007/s11214-015-0164-9

Burlaga, L. F., Ness, N. F., & Acúna, M. H. (2006). Trains of magnetic holes and magnetic humps in the heliosheath. *Geophysical Research Letters*, *33*, L21106. https://doi.org/10.1029/2006GL027276

Califano, F., Hellinger, P., Kuznetsov, E., Passot, T., Sulem, P. L., & Trávníček, P. M. (2008). Nonlinear mirror mode dynamics: Simulations and modeling. *Journal of Geophysical Research*, *113*, A08219. https://doi.org/10.1029/2007JA012898

Chisham, G., Burgess, D., Schwartz, S. J., & Dunlop, M. W. (1998). Observations of electron distributions in magnetosheath mirror mode waves. *Journal of Geophysical Research*, *103*, 26,765–26,774. https://doi.org/10.1029/98JA02620

Feygin, F. Z., Khabazin, Y. G., Simonenko, V. A., & Kondrat'ev, A. A. (2009). Linear theory of slow drift mirror kinetic instability at finite electron temperature. *Geomagnetism and Aeronomy*, *49*, 30–41.

Fu, H. S., Khotyaintsev, Y. V., André, M., & Vaivads, A. (2011). Fermi and betatron acceleration of suprathermal electrons behind dipolarization fronts. *Geophysical Research Letters*, *38*, L16104. https://doi.org/10.1029/2011GL048528

Fu, H. S., Khotyaintsev, Y. V., Vaivads, A., André, M., Sergeev, V. A., Huang, S. Y., et al. (2012). Pitch angle distribution of suprathermal electrons behind dipolarization fronts: A statistical overview. *Journal of Geophysical Research*, *117*, A12221. https://doi.org/10.1029/2012JA018141

Fu, H. S., Khotyaintsev, Y. V., Vaivads, A., Retinò, A., & André, M. (2013). Energetic electron acceleration by unsteady magnetic reconnection. *Nature Physics*, *9*, 426–430. https://doi.org/10.1038/NPHYS2664

Gary, S. P., & Karimabadi, H. (2006). Linear theory of electron temperature anisotropy instabilities: Whistler, mirror, and Weibel. *Journal of Geophysical Research*, *111*, A11224. https://doi.org/10.1029/2006JA011764

Gedalin, M., Lyubarski, Y. E., Balikhin, M., & Russell, C. T. (2001). Mirror modes: Non-Maxwellian distributions. *Physics of Plasmas*, *8*, 2934.

Genot, V., Budnik, E., Hellinger, P., Passot, T., Belmont, G., Travniek, P. M., et al. (2009). Mirror structures above and below the linear instability threshold: Cluster observations, fluid model and hybrid simulations. *Annales de Geophysique*, *27*, 601–615.

Hasegawa, A. (1969). Drift mirror instability in the magnetosphere. *Physics of Fluids*, *12*, 2642–2650. https://doi.org/10.1063/1.1692407

Hellinger, P., Kuznetsov, E. A., Passot, T., Sulem, P. L., & Trávníček, P. M. (2009). Mirror instability: From quasi-linear diffusion to coherent structures. *Geophysical Research Letters*, *36*, L06103. https://doi.org/10.1029/2008GL036805

Horbury, T. S., Lucek, E. A., Balogh, A., Dandouras, I., & Re'me, H. (2004). Motion and orientation of magnetic field dips and peaks in the terrestrial magnetosheath. *Journal of Geophysical Research*, *109*, A09209. https://doi.org/10.1029/2003JA010237

Istomin, Y. N., Pokhotelov, O. A., & Balikhin, M. A. (2009). Nonzero electron temperature effects in nonlinear mirror modes. *Physics of Plasmas*, *16*, 122901.

Ji, X.-F., Wang, X.-G., Sun, W.-J., Xiao, C.-J., Shi, Q.-Q., Liu, J., & Pu, Z.-Y. (2014). EMHD theory and observations of electron solitary waves in magnetotail plasmas. *Journal of Geophysical Research: Space Physics*, *119*, 4281–4289. https://doi.org/10.1002/2014JA019924

Joy, S. P., Kivelson, M. G., Walker, R. J., Khurana, K. K., Russell, C. T., & Paterson, W. R. (2006). Mirror-mode structures in the Jovian magnetosheath. *Journal of Geophysical Research*, *111*, A12212. https://doi.org/10.1029/2006JA011985

Kivelson, M. G., & Southwood, D. J. (1996). Mirror instability II: The mechanism of nonlinear saturation. *Journal of Geophysical Research*, *101*, 17,365–17,372. https://doi.org/10.1029/96JA01407

Klimushkin, D. Y., & Chen, L. (2006). Eigenmode stability analysis of drift-mirror modes in nonuniform plasmas. *Annales de Geophysique*, *24*, 2435–2439. https://doi.org/10.5194/angeo-24-2435-2006

Konjukov, M. V., & Terietskij, J. P. (1958). On the theory of the linear betatron [J]. *IL Nuovo Cimento*, *9*(6), 930–941.

Li, Z.-Y., Sun, W.-J., Wang, X.-G., Shi, Q.-Q., Xiao, C.-J., Pu, Z.-Y., et al. (2016). An EMHD soliton model for small-scale magnetic holes in magnetospheric plasmas. *Journal of Geophysical Research: Space Physics*, *121*, 4180–4190. https://doi.org/10.1002/2016JA022424

Liu, C. M., Fu, H. S., Cao, J. B., Xu, Y., Yu, Y. Q., Kronberg, E. A., & Daly, P. W. (2017). Rapid pitch angle evolution of suprathermal electrons behind dipolarization fronts. *Geophysical Research Letters*, *44*, 10,116–10,124. https://doi.org/10.1002/2017GL075007

Northrop, T. G. (1963). Adiabatic charged-particle motion. *Reviews of Geophysics*, *1*(3), 283–304. https://doi.org/10.1029/RG001i003p00283

Pantellini, F. G. E. (1998). A model of the formation of stable non-propagating magnetic structures in the solar wind based on the nonlinear mirror instability. *Journal of Geophysical Research*, *103*, 4789–4798. https://doi.org/10.1029/97JA02384

Pantellini, F. G. E., & Schwartz, S. J. (1995). Electron temperature effects in the linear proton mirror instability. *Journal of Geophysical Research*, *100*, 3539–3549. https://doi.org/10.1029/94JA02572

Pokhotelov, O. A., Balikhin, M. A., Alleyne, S. C. K., & Onishchenko, O. G. (2000). Mirror instability with finite electron temperature effects. *Journal of Geophysical Research*, *105*(A2), 2393–2401. https://doi.org/10.1029/1999JA900351

Pokhotelov, O. A., Onishchenko, O. G., & Stenflo, L. (2013). Physical mechanisms for electron mirror and field swelling modes. *Physica Scripta*, *87*(6), 065303.

Pokhotelov, O. A., & Pilipenko, V. A. (1976). Contribution to the theory of the drift-mirror instability of the magnetospheric plasma. *Geomagnetism and Aeronomy*, *16*, 296.

Pollock, C., Moore, T., Jacques, A., Burch, J., Gliese, U., Saito, Y., et al. (2016). Fast plasma investigation for magnetospheric multiscale. *Space Science Reviews*, *199*(1-4), 331–406. https://doi.org/10.1007/s11214-016-0245-4

Porazik, P., & Johnson, J. R. (2013a). Gyrokinetic particle simulation of nonlinear evolution of mirror instability. *Journal of Geophysical Research: Space Physics*. *118*, 7211–7218. https://doi.org/10.1002/2013JA019308

Porazik, P., & Johnson, J. R. (2013b). Linear dispersion relation for the mirror instability in the context of the gyrokinetic theory. *Physics of Plasmas*, *20*, 104,501.

Russell, C. T., Anderson, B. J., Baumjohann, W., Bromund, K. R., Dearborn, D., Fischer, D., et al. (2016). The Magnetospheric Multiscale magnetometers. *Space Science Reviews*, *199*(1-4), 189–256. https://doi.org/10.1007/s11214-014-0057-3

Russell, C. T., Mellott, M. M., Smith, E. J., & King, J. H. (1983). Multiple spacecraft observations of interplanetary shocks: Four spacecraft determinations of shock normals. *Journal of Geophysical Research*, *88*, 4739–4748.

Russell, C. T., Riedler, W., Schwingenshuh, K., & Yeroshenko, Y. (1987). Mirror instability in the magnetosphere of comet Halley. *Geophysical Research Letters*, *14*, 644.

Shi, Q. Q., Pu, Z. Y., Soucek, J., Zong, Q.-G., Fu, S. Y., Xie, L., et al. (2009). Spatial structures of magnetic depression in the Earth's high-altitude cusp: Cluster multipoint observations. *Journal of Geophysical Research*, *114*, A10202. https://doi.org/10.1029/2009JA014283

Shi, Q. Q., Shen, C., Dunlop, M. W., Pu, Z. Y., Zong, Q.-G., Liu, Z. X., et al. (2006). Motion of observed structures calculated from multi-point magnetic field measurements: Application to Cluster. *Geophysical Research Letters*, *33*, L08109. https://doi.org/10.1029/2005GL025073

Shi, Q. Q., Shen, C., Pu, Z. Y., Dunlop, M. W., Zong, Q.-G., Zhang, H., et al. (2005). Dimensional analysis of observed structures using multipoint magnetic field measurements: Application to Cluster. *Geophysical Research Letters*, *32*, L12105. https://doi.org/10.1029/2005GL022454

Soucek, J., & Escoubet, C. P. (2011). Cluster observations of trapped ions interacting with magnetosheath mirror modes. *Annales Geophysicae*, *29*, 1049–1060. https://doi.org/10.5194/angeo-29-1049-2011

Soucek, J., Lucek, E., & Dandouras, I. (2008). Properties of magnetosheath mirror modes observed by Cluster and their response to changes in plasma parameters. *Journal of Geophysical Research*, *113*, A04203. https://doi.org/10.1029/2007JA012649

Southwood, D. J., & Kivelson, M. G. (1993). Mirror instability. I—Physical mechanism of linear instability. *Journal of Geophysical Research*, *98*, 9181–9187. https://doi.org/10.1029/92JA02837

Treumann, R. A., Jaroschek, C. H., Constantinescu, O. D., Nakamura, R., Pokhotelov, O. A., & Georgescu, E. (2004). The strange physics of low frequency mirror mode turbulence in the high temperature plasma of the magnetosheath. *Nonlinear Processes in Geophysics*, *11*, 647–657.

Tsurutani, B. T., Richardson, I. G., Lepping, R. P., Zwickl, R. D., Jones, D. E., & Smith, E. J. (1984). Drift mirror mode waves in the distant (X~200 Re) magnetosheath. *Geophysical Research Letters*, *11*, 1102.

Tsurutani, B. T., Southwood, D. J., Smith, E. J., & Balogh, A. (1992). Nonlinear magnetosonic waves and mirror mode structures in the March 1991 ULYSSES interplanetary event. *Geophysical Research Letters*, *19*, 1267–1270. https://doi.org/10.1029/92GL00782

Xiao, T., Shi, Q. Q., Tian, A. M., Sun, W. J., Zhang, H., Shen, X. C., & Du, A. M. (2014). Plasma and magnetic-field characteristics of magnetic decreases in the solar wind at 1 AU: Cluster-C1 observations. *Solar Physics*, *289*(8), 3175–3195.

Yao, S., He, J.-S., Tu, C.-Y., Wang, L.-H., & Marsch, E. (2013). Small-scale pressure-balanced structures driven by mirror-mode waves in the solar wind. *The Astrophysical Journal*, *776*, 94. https://doi.org/10.1088/0004-637X/776/2/94

Yao, S. T., Shi, Q. Q., Guo, R. L., Yao, Z. H., Tian, A. M., Degeling, A. W., et al. (2018). Magnetospheric Multiscale observations of electron scale magnetic peak. *Geophysical Research Letters*, *45*, 527–537. https://doi.org/10.1002/2017GL075711

Yao, S. T., Shi, Q. Q., Li, Z. Y., Wang, X. G., Tian, A. M., Sun, W. J., et al. (2016). Propagation of small size magnetic holes in the magnetospheric plasma sheet. *Journal of Geophysical Research: Space Physics*, *121*, 5510–5519. https://doi.org/10.1002/2016JA022741

Yao, S. T., Wang, X. G., Shi, Q. Q., Pitkänen, T., Hamrin, M., Yao, Z. H., et al. (2017). Observations of kinetic-size magnetic holes in the magnetosheath. *Journal of Geophysical Research: Space Physics*, *122*, 1999–2000. https://doi.org/10.1002/2016JA023858

Zhang, T. L., Russell, C. T., Baumjohann, W., Jian, L. K., Balikhin, M. A., Cao, J. B., et al. (2008). Characteristic size and shape of the mirror mode structures in the solar wind at 0.72 AU. *Geophysical Research Letters*, *35*, L10106. https://doi.org/10.1029/2008GL033793